Conference Paper

Fluid Dynamics in Electrode Flushing Channel and Electrode-Workpiece Gap During EDM Drilling

Author(s):
Wegener, K.; Kliuev, Mikhail; Baumgart, Christoph

Publication Date:
2018

Permanent Link:

https://doi.org/10.3929/ethz-b-000280188 →

Originally published in:

Procedia CIRP 68, http://doi.org/10.1016/j.procir.2017.12.058 →

Available online at www.sciencedirect.com

ScienceDirect

Procedia CIRP 68 (2018) 254 – 259

www.elsevier.com/locate/procedia

19th CIRP Conference on Electro Physical and Chemical Machining, 23-27 April 2018, Bilbao, Spain

Fluid Dynamics in Electrode Flushing Channel and Electrode-Workpiece Gap During EDM Drilling

M. Kliuev[a]*, C. Baumgart[a], K. Wegener[a]

[a] *Institute of Machine Tools and Manufacturing (IWF), ETH Zürich, Switzerland*

* Corresponding author. Tel.: +41 44 632 32 51; fax: +41 44 632 11 25. *E-mail address:* klyuev@iwf.mavt.ethz.ch

Abstract

Evacuation of removed material is a key limitation factor in EDM drilling, as debris particles remaining in the gap between electrode and workpiece could reattach to the workpiece or cause ineffective discharges. In order to increase particle evacuation rate, electrodes with internal flushing channels are used. In this work, the influence of drilling conditions to the pressure drop and dielectric flow during EDM drilling is investigated analytically and through computational fluid dynamics (CFD) simulations. The electrode diameter, gap, configuration of the flushing channel, electrode length and drill depth are analysed to estimate and describe the influence on the flow. The change of flow with wearing out of the electrode needs to be taken into account. Also the configuration of the channel cross section has a great influence to the flow. Turbulences, pressure and velocity distribution are analysed through the numerical simulation. The gap between electrode and workpiece matters when the electrode is short and / or the drilling hole is deep. The flushing efficiency has a significant effect on the recast layer thickness (RLT), which can influence the workpiece quality. With the shortening of the electrode during the process the RLT is reduced by more than 15% with the faster dielectric flow, which has to be considered for achieving constant process conditions. The results of the simulations are compared and verified with drilling experiments by investigating the flow conditions as well as the process performance for various electrodes and the influence on the RLT.

Peer-review under responsibility of the scientific committee of the 19th CIRP Conference on Electro Physical and Chemical Machining

Keywords: Electrical Discharge Machining (EDM), EDM drilling, computational fluid dynamics (CFD);

1. Introduction

Nearly all electrodes used for EDM drilling have internal flushing channels. Especially in deep hole drilling flushing of dielectric fluid through those channels is practically the only one effective method to evacuate removed material.

One of the biggest limitations during deep hole drilling is caused by side electrode wear induced by lateral sparks, which is also promoting electrode vibration. Vibrations and therefore wear increase with the aspect ratio between electrode diameter and hole depth.

Insufficient flushing increases the probability of lateral sparks and slows down the removed material evacuation, where the flushing efficiency depends on electrode length and geometry, hole depth and initial pressure.

Nomenclature

ρ	density of the fluid [kg/m^3]
v	velocity of the fluid with respect to the object [m/s]
l	linear dimension [m]
L	characteristic length [m]
μ	dynamic viscosity of the fluid [Pa·s or kg/(m·s)]
Q	volumetric flow rate [m^3/s]
r	radius [m]
Δp	pressure difference [Pa]
ε	sand-grain roughness [μm]
H	Feed of the electrode, which is set as the parameter on the EDM machine and the electrode wear is not compensated

Peer-review under responsibility of the scientific committee of the 19th CIRP Conference on Electro Physical and Chemical Machining
doi:10.1016/j.procir.2017.12.058

1.1. Electrode types comparison

Multi-channel electrodes are mainly used for blind-hole drilling, whereas single-channel electrode cannot be used because of spike creation in the center of the hole. Various internal channel configurations of multi-channel electrodes exist depending on the diameter and electrode manufacturer.

Depending on the application flushing could be streamed through single or multi-channel electrodes. Comparison between single-channel and multi-channel electrodes was made by Yilmaz [1] and by Bozdana [2]. In these works different channel configurations were used. This fact leads Yilmaz and Bozdana to contradictory results. Bozdana showed higher material removal rate (MRR) with multi-channel electrode, while Yilmaz considered higher MRR with single-channel electrode. Various MRRs were caused by different channel configurations used by Yilmaz and Bozdana proving the significance of multi-channel configuration and its influence to the process outputs. Different multi-channel electrode configurations are shown in Fig. 1. The design of the cross section highly influences the flow conditions as the flow regime and the pressure drop can rise and these factors influence flushing.

Fig. 1. Multi-channel channel configuration comparison [1-3]. Type 1 is used for flow simulation, this type is recommended by machine tool manufacturer.

Cylindrical electrodes without channels are widely used in die sinking, where flushing originates in periodic electrode movement. Special electrode types e.g. helical electrodes and etc. can be beneficial for certain applications. Plasa [4] showed that the use of helical electrodes is reasonable for deep hole machining in Ti6Al4V. However helical electrodes are expensive in production.

1.2. CFD simulations in EDM

The largest number of CFD simulations in EDM is performed for die-sinking process in oil dielectric. Eroded particles and bubbles distribution were studied by Pontelandolfo [5], where the author was working on homogeneous distribution of the eroded material in a dielectric. He found that bubbles are increasing the evacuation rate of the removed material. Wang and Han [6] were researching bubbles and debris movement. They found out that electrode jump height is influencing the amount of clean oil in the electrode-workpiece gap, therefore the electrode jump speed is influencing removed material distribution.

High-speed camera observation of bubbles was made by Maradia [7]. Maradia investigated bubble dynamics in micro-/meso-/macro scale. In micro-scale the discharge forces the gas bubble displacement, while in meso-/macro scale the bubble remains in the discharge region.

Wang [8] simulated liquid-solid two-phase flow through the single-channel electrode during EDM drilling process in deionized water. Wang showed, that concentration of the debris particles is higher around the corner in the machined hole. The dielectric pressure was reducing along with electrode length.

2. Flow analysis in electrode flushing channel

2.1. Reynolds number calculation

In order to calculate the flow conditions the flow regime has to be estimated by using the Reynolds number, which is defined in Eq. (1):

$$\mathrm{Re} = \frac{\rho \cdot v \cdot L}{\mu} \tag{1}$$

In a cylindrical tube flow the transition from laminar to turbulent flow is considered at a Reynolds number of about 2300. The characteristic length is chosen as the inner diameter of the tube respectively the diameter of the largest possible inscribed circle of the multi-channel tube. Water data at 25 °C is used and has a density ρ=997 kg/m^3 and dynamic viscosity μ=8.9·10^{-4} kg/(m·s), while the velocity depends on the electrode length for the given input pressure of p=6.5 MPa and is read from the simulation results, which are discussed in more detail in the next section. Table 1 shows the expected flow conditions for the investigated electrodes depending on the chosen electrode as well as their length.

Table 1. Reynolds numbers estimation.

Electrode type	characteristic length L [mm]	Reynolds number, l=100 mm	Reynolds number, l=400 mm
Multi-channel 1.0 mm	0.2	5130	2490
Multi-channel 0.5 mm	0.1	1700	880
Single-channel 0.5 mm	0.2	992	744

While the 0.5 mm outer-diameter electrodes show Reynolds numbers below 2300, the calculated Reynolds number for the 1.0 mm multi-channel electrode is above 2300 and even for the longer electrode, which usually shows lower velocities due to the higher pressure drop. Thus the flow can be simulated assuming laminar flow conditions for the 0.5 mm electrodes while for the 1.0 mm electrode turbulence models are applied.

2.2. Hagen-Poiseuille law

Considering laminar flow conditions in a circular tube, the Hagen-Poiseuille law, which is showed in Eq. (2), can be used to estimate analytically the mean flow rate or flow velocity in the electrodes based on the provided pressure from the machine.

$$Q = \frac{\pi \cdot \Delta p \cdot r^4}{8 \cdot \mu \cdot l} \tag{2}$$

The flow rate is in inverse proportion to the length of the electrode but proportional to the radius to the power of four. An electrode which is worn down to half of its length will provide doubled flow rate. On the other hand the cross section of the electrode influences the flow rate. To investigate the conditions of multi-hole configurations fluid flow simulations are conducted. The performance of the process is depending strongly on the removal of the debris, which is highly influenced by the flushing and thus the flow rate of the dielectric out of the electrode.

3. Fluid flow simulation

3.1. Surface roughness and sand-grain roughness

As the 1.0mm multi-hole configuration electrode needs to be simulated by employing turbulence models the wall roughness needs to be estimated. Beside the no slip condition, which means flow velocity of zero at the walls, the roughness is used to calculate the wall flow profile close to the wall. To include the roughness inside electrode chambers and the drilled hole in the simulation the relation between ten-point mean roughness Ra and sand-grain roughness is used. The relation was empirically found by Adams in [9] and shown in Eq. (3).

$$\varepsilon = 5.863\mathrm{Ra} \tag{3}$$

Measured Ra roughness and calculated sand-grain roughness are shown in Table 2.

Table 2. Ra roughness and sand-grain roughness.

Roughness	Inside of electrodes channel	Outer electrode surface	The surface of hole
Ra [µm]	1	6.4	6.4
ε [µm]	5.86	37.52	37.52

Talysurf from Taylor Hobson is used for tactile measurements of the roughness. For CFD simulations ANSYS 18.1 is used, while the geometry files are made with SolidWorks 2016 in analogy to the experimental set-up. The cross-section of the multi-hole electrode was determined by an Alicona measurement with a slightly simplified inner geometry at the corners to mesh the model. The standard k-ε-model for turbulence is applied. Due to the small geometry features of the multi-hole electrode a rather fine mesh consisting of 200’000-1’000’000 cells, depending on the size and length of the electrode, is used to resolve the flow profile over the cross section.

3.2. Single-channel electrode

The single-channel electrode flow can be treated as the well-known flow through a cylindrical tube. From experience and analytical investigation a circular cross-section offers the best geometry for lower pressure drop. The flow profile of the fully developed laminar flow can be assumed to be parabolic. Tietjens [10] proposed for the entry length for a stabile laminar flow the following relation:

$$l_{entry} = 0.06 \cdot \mathrm{Re} \cdot \mathrm{L} \tag{4}$$

Thus for the short single hole electrode an entry length of about 12 mm for a fully developed flow is estimated.

3.3. Multi-channel electrode

In order to study the multi-channel electrode flow computational flow simulations become more important, as the geometry is more complex. Fig. 2 shows on the left side the velocity distribution of the 1.0mm multi-hole electrode, while due to the turbulent flow conditions high velocity gradients towards the wall occur. On the right side the turbulent kinetic energy distribution is shown, which reaches the maxima close to the center walls. The volume flow rate is about factor eight times smaller compared to the single hole electrode due to cross-section and velocity profile.

Fig. 3 is showing the cross-section into the lower part of the multi-hole configuration electrode in a workpiece for the turbulent kinetic energy distribution (YZ-plane). It can be observed, that the highest distortions occur in the corner of the gap, where the flow changes its direction. Due to the pressure drop lower flow rates are measured, where shorter electrodes have a much higher influence compared to longer ones (25% to almost zero) due to the lower flow speed, which is shown in more detail in chapter 4.

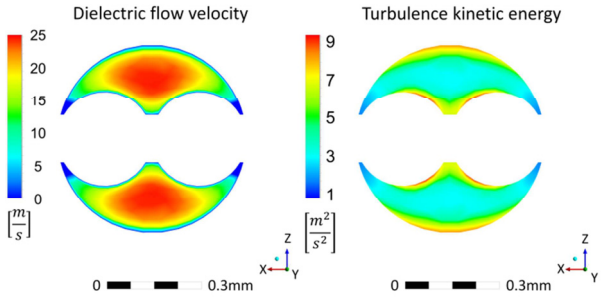

Fig. 2. Axial flow velocity distribution at the outlet (left) and turbulence kinetic energy at the outlet (right) of a type 1 (Fig 1), 1.0mm outer diameter multi-hole electrode, where turbulent flow conditions are considered

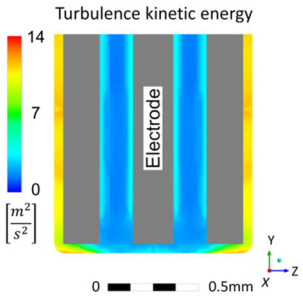

Fig. 3. Turbulence kinetic energy plot in cross-section of YZ-plane of the lower part of the multi-hole electrode insertion into the workpiece gap

4. Results and verification

4.1. Experiment setup for high speed camera observation

In order to investigate flow dynamics and influence of electrical discharge on the flow, a high-speed camera Phantom v12.1 from Vision Research is used. The image recording frame rate is set to 30000 fps. The experiments are performed on Drill 300 from GFMS. The experimental setup is shown in Fig. 4.

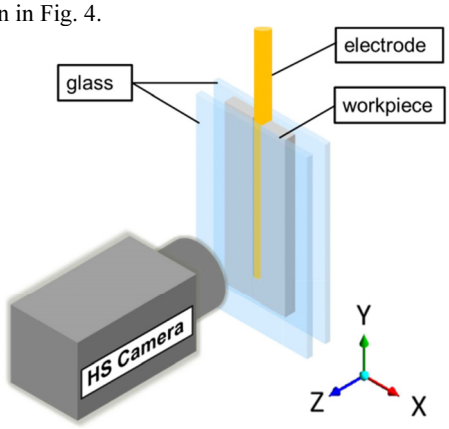

Fig. 4. High speed camera setup, the workpiece is mounted between two pieces of glass

The workpiece is clamped between pieces of glass in order to be observed by the camera. Light sources are used from the front and from the back sides. An electrode is placed in the cuboidal 12 mm long slot, which is machined in Inconel 718. Observations are made with 0.5 mm multi-channel and single-channel electrodes.

4.2. High speed camera observation

The velocity of the flow is analysed based on tracking of bubble movement. Of course the movement of bubbles is not equal to the flow velocity, however, the flow velocity influences the velocity of the bubble. Fig. 5 and Fig. 6 show the bubble movement with single-channel and multi-channel electrodes.

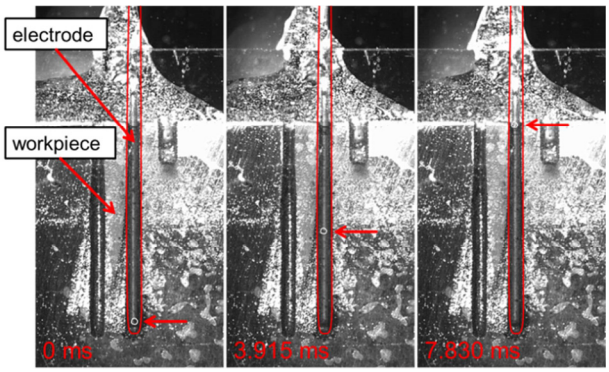

Fig. 5. High speed tracking of the bubble movement with 0.5 mm single-channel electrode. The stream of water is visible above the hole.

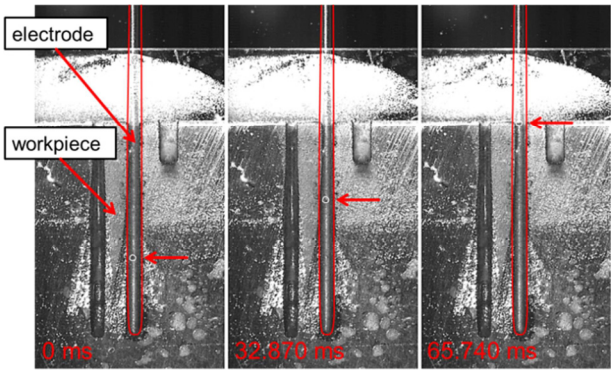

Fig. 6. High speed tracking of the bubble movement with 0.5 mm multi-channel electrode

The bubble tracing showed, that the flow velocity with the multi-channel electrode is significantly lower in comparison to the single-channel electrode. The experiment was repeated with and without erosion. Discharges do not have a significant influence on the bubble movement; however the movement of the single-bubble is no longer possible to track, since far more bubbles are created. Nevertheless the discharge should have an influence to the flushing conditions and this influence is probably not visible since a cuboidal hole is used for observation.

The bubble, created during the discharge in water is very different to the bubble in oil, which was mostly analyzed in the literature. After the discharge collapse the bubble gets split into numerous small bubbles, while in oil single bubble remains. Small bubbles are evacuated faster and do not significantly interfere the erosion process.

4.3. Volume flow rate measurements

The flow rate of a 1 mm multi-channel electrode type 1 (see Fig. 1) is measured and simulated in- and outside of a workpiece, whereas the results are shown in Fig. 7. Generally the flow through the electrode inside the workpiece, is slower due to higher pressure drop, which is induced at the walls of the workpiece and due to the change of flow direction and cross section. The difference is higher when the flow rate is higher than 1 ml/sec, where it can be caused by a higher pressure drop due to turbulence, considering a non-linear problem. The influence of the electrode length on the flow rate is significant. A 100 mm electrode has a three to four times higher flow rate as a 400 mm long electrode.

Experimental flow rate is usually higher than the simulated one due to the unknown pressure drop through the variation in the cross section of the small electrodes and from the measurement at the pump to the electrode. The pressure drop from the pump to the electrode is supposed to be small considering Hagen-Poiseuille law, as the flow rate is very low and the diameter of the ducts from the pump are larger compared to the electrode channels. Finally the properties of the fluid are supposed to be the ones of clean water without particles. To improve the model an accurate measurement of the pressures as well as the electrode geometry over the whole length is recommended.

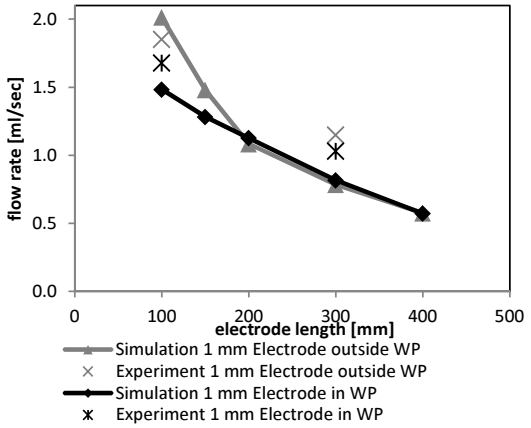

Fig. 7. Flow rate through the 1 mm diameter multi-channel electrode 10 mm inside the workpiece (WP) and outside the workpiece, simulation and experiment.

Table 3. Flow rate measurements and simulation for 1 mm multi-channel, 0.5 mm single/multi-channel electrodes outside workpiece.

	Experiment		Simulation				
Electrode length [mm]	100	300	100	150	200	300	400
1 mm electrode outside work-piece [ml/sec]	1.85	1.15	2.01	1.48	1.08	0.78	0.58
1 mm electrode inside work-piece [ml/sec]	1.68	1.03	1.48	1.28	1.13	0.82	0.57
0.5 mm multi-channel electrode [ml/sec]	0.08*	0.045*	0.61	0.75	0.40	0.41	0.31
0.5 mm electrode single -channel [ml/sec]	0.78	0.37	0.81	0.60	0.49	0.35	0.25

* For 0.5 mm multi-channel electrode experiments are made with 200 mm and 400 mm electrode length.

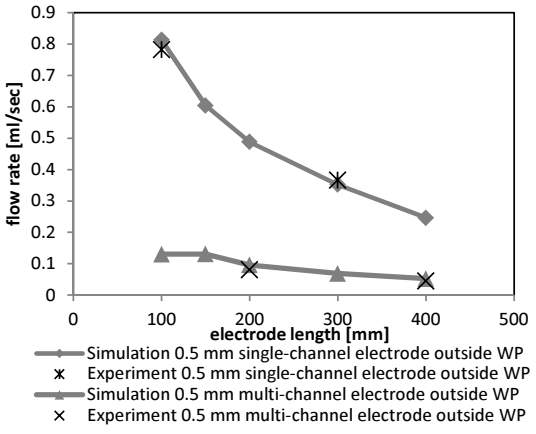

Fig. 8. Flow rate through the 0.5 mm diameter single-channel electrode for 10 mm inside the workpiece (WP), simulation and experiment

4.4. MRR and Electrode wear

In order to see the effect of flushing to MRR and relative electrode wear (E_W) the drilling tests are performed. Electrode wear measurement E_{Wt} is performed after every erosion and it is considered as reduction of the length of the electrode. From those measurements the relative tool wear is calculated as wear related to the eroded workpiece volume,

$$E_W = \frac{E_{Wt}}{H - E_{Wt}} \cdot 100\% \tag{4}$$

where E_{Wt} is the total reduction of electrode length, which is measured automatically by the machine. Material removal rate MRR is calculated as:

$$MRR = \frac{(H - E_{Wt}) \cdot \mathrm{A}}{t} \tag{5}$$

where t is the machining time and A is the area of hole.

Experimental data regarding MRR and electrode wear is shown in Table 4. Experiment conditions and erosion parameters are in Table 5.

Table 4. MRR measurements.

Electrode diameter	Electrode length [mm]	E_w [%]	MRR [mm^3/s]
1 mm multi-channel	200	34.2	2.83
	400	33.96	2.76
0.5 mm multi-channel	200	37.0	0.33
	400	95.2	0.15
0.5 mm single-channel	200	125.4	0.76
	400	155.0	0.70

For 0.5 mm multi-channel electrode the discharge current is significantly reduced, due to electrode destruction through melting. Thereby internal flushing has also electrode cooling function, which is important for thin electrodes, where electrical resistivity is high.

Experiments showed that MRR is not significantly influenced by fluid flow reduction for 1 mm multi-channel and 0.5 mm single-channel electrodes. However with the shorter electrode slight increase of MRR is seen.

The electrode wear significantly reduces along with the electrode length reduction for the 0.5 mm single-channel electrode and even more for the 0.5 mm multi-channel electrode. The influence of electrode length to MRR is insignificant with 1 mm electrode.

As it is previously shown, the 0.5 mm multi-channel electrode has the most significant drop of flushing flow with the length. This fact leads to almost linear increase of MRR along with the electrode length reduction. The electrode wear with long 0.5 mm diameter multi-channel electrodes is almost three times higher than with short electrodes. If flushing efficiency is insufficient to remove the eroded material from

the hole, it will lead to ineffective discharges. The increase of pause duration will probably help to evacuate the eroded material, which will not increase the MRR, but will help to decrease E_w and enhance the process stability.

Table 5. EDM conditions

	EDM Condition
Workpiece material	Inconel 718
Electrode material	Copper
Dielectric	Deionized water
Holes type	Blind
Pause duration	15 µs
Ignition voltage	120 V
Pulse duration	32 µs
Discharge current	28 A, 14 A*
H	10 mm
Dielectric pressure	6.5 MPa
Electrode polarity	negative

* Lower discharge current is applied for 0.5 mm multi-channel electrode

4.5. Recast layer measurements

The recast layer thickness (RLT) measurements are presented in Table 6. The flushing conditions have an influence on the RLT with both 1mm multi-channel and 0.5 mm single-channel electrodes. However the difference is much higher with smaller electrodes. A higher RLT in case of 0.5 mm electrodes can be caused by a smaller electrode-workpiece gap and not by internal electrode flushing. The method and preparations for recast layer measurements are shown in [3].

Table 6. Recast layer measurements.

Electrode length [mm]	Measuring site	RLT 1 mm electrode [µm]	RLT 0.5 mm electrode [µm]
200	entrance	18.9	12.7
200	exit	18.9	17.8
400	entrance	19.2	15.3
400	exit	20.5	24.6

RLT seems to be the most significant output, influenced by the flow rate reduction.

5. Conclusions

The internal flushing channel diameter and configuration have a significant effect on the flushing speed and efficiency of debris particle removal. The effect is particularly important for small diameter electrodes and complex multi-channel electrodes. For such electrodes flushing can be insufficient to evacuate eroded material, which will lead to ineffective discharges, where MRR is low and E_w is high.

It is clearly seen, that the flow velocity is influenced by the high aspect ratio between hole diameter and hole depth. Flow simulations have been used to compare the flow rates of the different electrodes, where the relation between length and flow rate can be confirmed and also complex cross sections of multi-hole electrodes can be investigated.

Insufficient flushing has also a tendency to increase the recast layer thickness, the effect is significant for high aspect ratios between hole diameter and hole depth. The effect needs to be taken into account, since RLT is the key limitation factor of EDM drilling application in aerospace.

High speed observations showed that the bubbles, created during the discharge in water, are very different to the bubbles in oil. In water, instead of one big bubble, numerous small bubbles are created. Small bubbles do not significantly interfere the erosion process.

Summarising, insufficient flushing efficiency is the key limitation factor in deep hole drilling. In this case, simple cylindrical flushing channel provides the best performance of the flow. Furthermore better flushing is not only enhancing the abilities of deep hole drilling and increasing MRR, but it is also reducing the recast layer thickness.

Acknowledgements

This study has been provided with the financial support of the Commission for Technology and Innovation CTI, Switzerland.

References

[1] Yilmaz O, Okka MA. Effect of single and multi-channel electrodes application on EDM fast hole drilling performance. The International Journal of Advanced Manufacturing Technology. 2010;51:185-94.

[2] Bozdana AT, Ulutas T. The Effectiveness of Multichannel Electrodes on Drilling Blind Holes on Inconel 718 by EDM Process. Materials and Manufacturing Processes. 2016;31:504-13.

[3] Kliuev M, Boccadoro M, Perez R, Dal Bó W, Stirnimann J, Kuster F, Wegener K. EDM Drilling and Shaping of Cooling Holes in Inconel 718 Turbine Blades. Procedia CIRP. 2016;42:322-7.

[4] Plaza S, Sanchez JA, Perez E, Gil R, Izquierdo B, Ortega N, Pombo I. Experimental study on micro EDM-drilling of Ti6Al4V using helical electrode. Precision Engineering. 2014;38:821-7.

[5] Pontelandolfo P, Haas P, Perez R. Particle Hydrodynamics of the Electrical Discharge Machining Process. Part 2: Die Sinking Process. Procedia CIRP. 2013;6:47-52.

[6] Wang J, Han F, Cheng G, Zhao F. Debris and bubble movements during electrical discharge machining. International Journal of Machine Tools and Manufacture. 2012;58:11-8.

[7] Maradia U, Wegener K, Stirnimann J, Knaak R, Boccadoro M. Investigation of the Scaling Effects in Meso-Micro EDM. 2013:V02BTA038.

[8] Y.Q. Wang MRC, Sheng Qiang Yang, Wen Hui Li. Numerical Simulation of Liquid-Solid Two-Phase Flow Field in Discharge Gap of High-Speed Small Hole EDM Drilling. Advanced Materials Research. 2008; Vols. 53-54:pp. 409-14.

[9] Adams T, Grant C, Watson H. A simple algorithm to relate measured surface roughness to equivalent sand-grain roughness. Journal ISSN. 2012; 2929:2724.

[10] Sigloch H. Technische Fluidmechanik. Springer-Vieweg: Berlin Heidelberg; 2014.